NAVAL POSTGRADUATE SCHOOL
Monterey, California

THESIS

19980414 046

MONITORING TEMPERATURE VARIABILITY ALONG THE CALIFORNIA COAST USING ACOUSTIC TOMOGRAPHY

by

Thierry Morvillez

September, 1997

Thesis Advisor: Ching-Sang Chiu
Co-Advisor: Curtis A Collins

Approved for public release; distribution is unlimited.

REPORT DOCUMENTATION PAGE

Form Approved
OMB No. 0704-0188

1. AGENCY USE ONLY *(Leave blank)*	2. REPORT DATE September 1997	3. REPORT TYPE AND DATES COVERED Master's Thesis

4. TITLE AND SUBTITLE **MONITORING TEMPERATURE VARIABILITY ALONG THE CALIFORNIA COAST USING ACOUSTIC TOMOGRAPHY**	5. FUNDING NUMBERS
6. AUTHOR(S) Thierry MORVILLEZ	
7. PERFORMING ORGANIZATION NAME(S) AND ADDRESS(ES) Naval Postgraduate School Monterey, CA 93943-5000	8. PERFORMING ORGANIZATION REPORT NUMBER
9. SPONSORING / MONITORING AGENCY NAME(S) AND ADDRESS(ES)	10. SPONSORING / MONITORING AGENCY REPORT NUMBER

11. SUPPLEMENTARY NOTES
The views expressed in this thesis are those of the author and do not reflect the official policy or position of the Department of Defense or the U.S. Government.

12a. DISTRIBUTION / AVAILABILITY STATEMENT	12b. DISTRIBUTION CODE
Approved for public release; distribution unlimited.	

13. ABSTRACT *(maximum 200 words)*

The electronic emissions of a low-frequency sound source placed by the Acoustic Thermometry of Ocean Climate (ATOC) project on Pioneer Seamount were monitored by a bottom-lying receiver on Sur Ridge from April 1996 to February 1997. The processed signals show a stable arrival pattern that was repeated in all the transmissions during the 11 months. Using the processed data, a tomographic analysis to study the coastal ocean variability along this California transmission path was conducted. Systematically, the analysis involved forward acoustic modeling of the arrival structure using ray theory, associating the observed arrivals with the modeled arrivals, extracting the travel times of the arrivals, inverting the travel times for temporal and spatial temperature changes, and interpreting the observed temperature variations. In particular, the tomographic estimate was compared to the temperature and wind measurements from an in situ mooring deployed by the Monterey Bay Aquarium Research Institution (MBARI). The comparison show that the tomographic estimate is of high quality and that the observed temperature variations were linked to coastal upwelling and downwelling events. The data, methods and result, demonstrating fully the feasibility of using tomography to study coastal temperature variability in central California on a long-term basis, are presented.

14. SUBJECT TERMS Tomography, Oceanography, Monterey Bay,			15. NUMBER OF PAGES 50
			16. PRICE CODE
17. SECURITY CLASSIFICATION OF REPORT Unclassified	18. SECURITY CLASSIFICATION OF THIS PAGE Unclassified	19. SECURITY CLASSIFI- CATION OF ABSTRACT Unclassified	20. LIMITATION OF ABSTRACT UL

NSN 7540-01-280-5500

Standard Form 298 (Rev. 2-89)
......................Prescribed by ANSI Std. 239-18

Approved for public release; distribution is unlimited

MONITORING TEMPERATURE VARIABILITY ALONG THE CALIFORNIA COAST USING ACOUSTIC TOMOGRAPHY

Thierry Morvillez
Lieutenant Commander, French Navy
B. S., French Naval Academy, 1978

Submitted in partial fulfillment of the
requirements for the degree of

MASTER'S OF SCIENCE IN PHYSICAL OCEANOGRAPHY

from the

NAVAL POSTGRADUATE SCHOOL
September 1997

Author: ______________________________
Thierry MORVILLEZ

Approved by: ______________________________
Ching-Sang Chiu, Thesis Advisor

____
Curtis A. Collins, Co Advisor

____
Robert H. Bourke, Chairman
Department of Oceanography

ABSTRACT

The electronic emissions of a low-frequency sound source placed by the Acoustic Thermometry of Ocean Climate (ATOC) project on Pioneer Seamount were monitored by a bottom-lying receiver on Sur Ridge from April 1996 to February 1997. The processed signals show a stable arrival pattern that was repeated in all the transmissions during the 11 months. Using the processed data, a tomographic analysis to study the coastal ocean variability along this California transmission path was conducted. Systematically, the analysis involved forward acoustic modeling of the arrival structure using ray theory, associating the observed arrivals with the modeled arrivals, extracting the travel times of the arrivals, inverting the travel times for temporal and spatial temperature changes, and interpreting the observed temperature variations. In particular, the tomographic estimate was compared to the temperature and wind measurements from an in situ mooring deployed by the Monterey Bay Aquarium Research Institution (MBARI). The comparison show that the tomographic estimate is of high quality and that the observed temperature variations were linked to coastal upwelling and downwelling events. The data, methods and result, demonstrating fully the feasibility of using tomography to study coastal temperature variability in central California on a long-term basis, are presented.

TABLE OF CONTENTS

ACKNOWLEDGMENTS

I would like to take this opportunity to express my sincere gratitude and appreciation to those who helped me throughout this thesis project. Firstly, I thank Professor Ching-Sang Chiu for his essential help in acoustic modeling, and guidance through the thesis process. Secondly, I thank my thesis Co-Advisor, Dr. Curt Collins for his help on this project. I would like to give very special thanks to Mr. Chris Miller, COACt Lab Manager, for his cooperation and assistance in processing the tomography data. Also, I would like to thank Mr. Rob Bourke for his assistance with writing in the English language.

I wish to gratefully acknowledge the permission of the ATOC project (Dr. Andrew Forbes)to utilize the Pioneer Seamount ATOC transmissions. Additionally, I would like to acknowledge the Monterey Bay Aquarium Research Institute for providing OASIS mooring data. Without the contributions of both of these organizations this thesis would not have been possible.

Finally, and most importantly, I thank my wife, Beatrice, and my six children for their steadfast support throughout the entire graduate school experience. I could not have completed my studies without their continuous patience, sacrifice, and love.

I. INRODUCTION

A. CENTRAL CALIFORNIA OCEANOGRAPHY

The California coast, particularly in the vicinity of the Monterey Bay is an oceanographically complex region. Different kinds of environmental conditions and air-sea interactions affect the water masses. The most common is upwelling, which brings cold nutrient rich water and a quasi-permanent fog to this area nearly all year long. As an eastern boundary, there is the cold, near-surface California current flowing to the South, and inshore and undercurrents flowing to the North. At variable time scales, El Nino events can significantly alter the regional oceanographic conditions. This is typified by a pronounced warming of the water column to great depths. While the deep submarine canyon modifies the local circulation and impacts tidal motion, insolation and wind patterns influence the mixed layer depth at hourly, daily or seasonal rhythms. All these factors make the measurement and understanding of the multiple-scale coastal ocean variability a difficult task.

A long term ocean temperature survey over a large area can enable us to study the trends and fluctuations along the coast, both the short-term variability linked to atmospheric disturbances and long-term evolution linked to the global climate change. Resolving the trends and fluctuations are fundamental to ocean process studies and, in the long run, ocean prediction.

As the atmospheric processes are better understood due to the ability of satellites to observe the entire atmosphere, only the very surface of the ocean is sensed by the satellite. The ocean stands as an opaque medium difficult to observe entirely from above (Robinson, 1985). By running numerical models which assimilate satellite altymetry like SOAP93 experiment, we have an approximate idea of the ocean variability. To improve this approximation, the models desperately need adequate in situ observations for improved initialization, calibration and validation. Interior observations that span long distances and a long time can come from acoustic tomography.

B. ACOUSTIC TOMOGRAPHY

Sound speed change is mainly a function of temperature variation. As we are able to accurately synchronize with great precision the emitter and receiver over great distances and knowing their fixed positions, the travel time of an emission is measured precisely. Transmitting periodically enables us to observe travel time changes. These changes reflect the variations of ocean temperature along the path. This is the basic principle of ocean acoustic tomography (Munk and Wunsch, 1979). Acoustic tomography also uses the acoustic multipaths to obtain vertical and horizontal resolution in a vertical plane.

Complementary to point measurements, acoustics measure the temperature variability that is integrated along a path. For this reason the Acoustic Thermometry of Ocean Climate (ATOC) project was launched in 1995 to monitor "average" temperatures in the Pacific Ocean. The emissions of an ATOC sound source located at the Pioneer Seamount were recorded at the Naval Postgraduate School Ocean Acoustic Observatory (NPS OAO). Since both the source and receiver are located on the coast of California, this opportunistic data set provides an occasion to study the temperature variability in the Monterey Bay National Marine Sanctuary over a period of eleven months.

C. THESIS OBJECTIVE AND APPROACH

The primary objective of this thesis is to study the temperature variability along the California coast using the tomographic data recorded at the NPS OAO from 20 April 1996 to 17 January 1997. During this period, the ATOC sound source north of the NPS OAO, emitted tomographic signals intermittently. Although the data gaps prevent a detailed interpretation of the fast temperature fluctuations along the coast, the data time series has enough quality to allow for an analysis of the slow fluctuations. Together with the temperature and wind data obtained by a hydrographic mooring, deployed by the Monterey Bay Aquarium Research Institution (MBARI) in the vicinity of the acoustic path, the Pioneer-to-Pt. Sur transmission has permitted an in-depth evaluation of the feasibility of using acoustic tomography for ocean monitoring in a coastal environment with a highly variable bathymetry.

Briefly, the analysis of the tomography data involved three major steps:

1. Forward Modeling. Acoustic propagation modeling was first performed to predict the basic pattern of ray arrivals at the NPS OAO receiver. The acoustic modeling used a ray theory approach that incorporated a "background" sound speed profile derived from a hydrographic survey conducted by Collins et al. (1997) and high-resolution bathymetry data. The predicted arrival pattern was then compared to the observed pattern for

validating the model results and associating the observed arrivals with the predicted eigenrays, a process known as ray identification.

2. Data Time Series Construction. Time series of stable and strong ray arrivals from the data were extracted and the corresponding travel times estimated. A low-order polynomial was then used to interpolate through the data gaps and, at the same time, filter out fast oscillations.

3. Inverse Analysis. The time series of filtered ray travel times were "inverted" using a minimum mean-square-error estimator. While the vertical structure was constrained by an empirical orthogonal mode (EOF) derived using the temperature data from the MBARI mooring, the temporal and horizontal structure of the temperature along the acoustic path was estimated at high resolution. The validation of the quality of the inverse solution and the oceanographic interpretation were aided with the hydrographic data from the MBARI mooring.

D. THESIS OUTLINE

A discussion of the acoustic tomography and hydrographic measurements used in this thesis research is presented in Chapter II. The forward modeling results as well as the extracted data series of ray travel times are presented in Chapter III. Chapter IV presents the inverse tomographic solution and includes a discussion of the horizontal resolution of the tomographic estimate, a comparison of the results to the moored hydrographic data and a physically oceanographic interpretation of the observed variability. Conclusions are given in Chapter V.

II. OBSERVATIONS

A. ACOUSTIC TOMOGRAPHY

1. Configuration

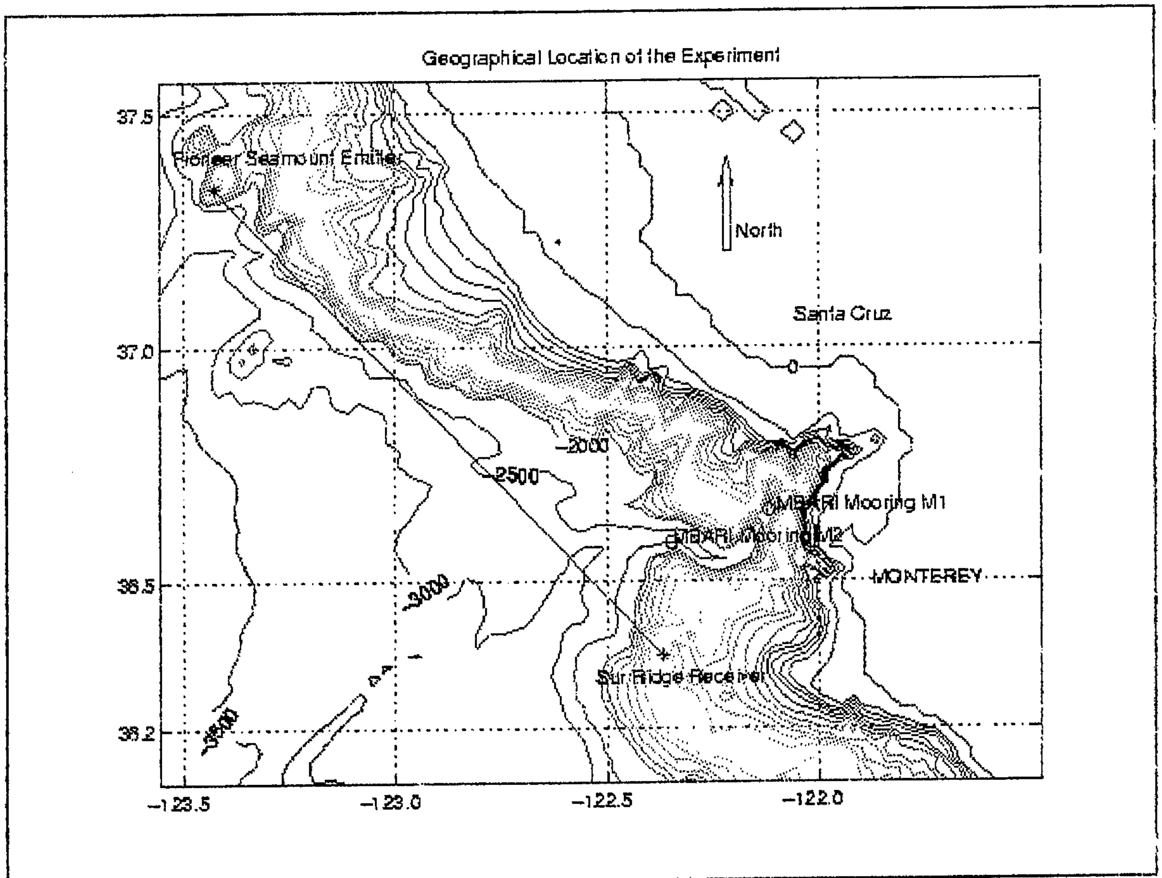

Figure 1. Bathymetric chart of the experimental region describing the location of the ATOC transmitter, NPS OAO receiver and MBARI moorings. Contours intervals are 100 m from 0 to 2000 m and 500 m from 2000 m to 3500 m.

Acoustic Thermometry of Ocean Climate (ATOC) (Munk et al., 1995) is a project measuring the travel time of an transmission from an acoustic projector to receivers throughout the Pacific ocean over a very long period. As travel time is directly related to the ocean temperature, ATOC is designed to monitor long-scale, long-term trends that are linked to climate change and global warming. One transmitter is located on

Pioneer Seamount which transmitted tomographic signals intermittently over a test period of 11 months. The transmissions were monitored by the NPS OAO with a receiver located at Sur Ridge. This study exploits those ATOC transmissions although it is not part of ATOC. As seen in Fig. 1, this data set recorded at NPS OAO provides for an excellent opportunity to study the coastal circulation of Central California. The track is only 160 km long, over highly variable bathymetry, presenting an acoustically challenging environment for applying the acoustic tomography technique.

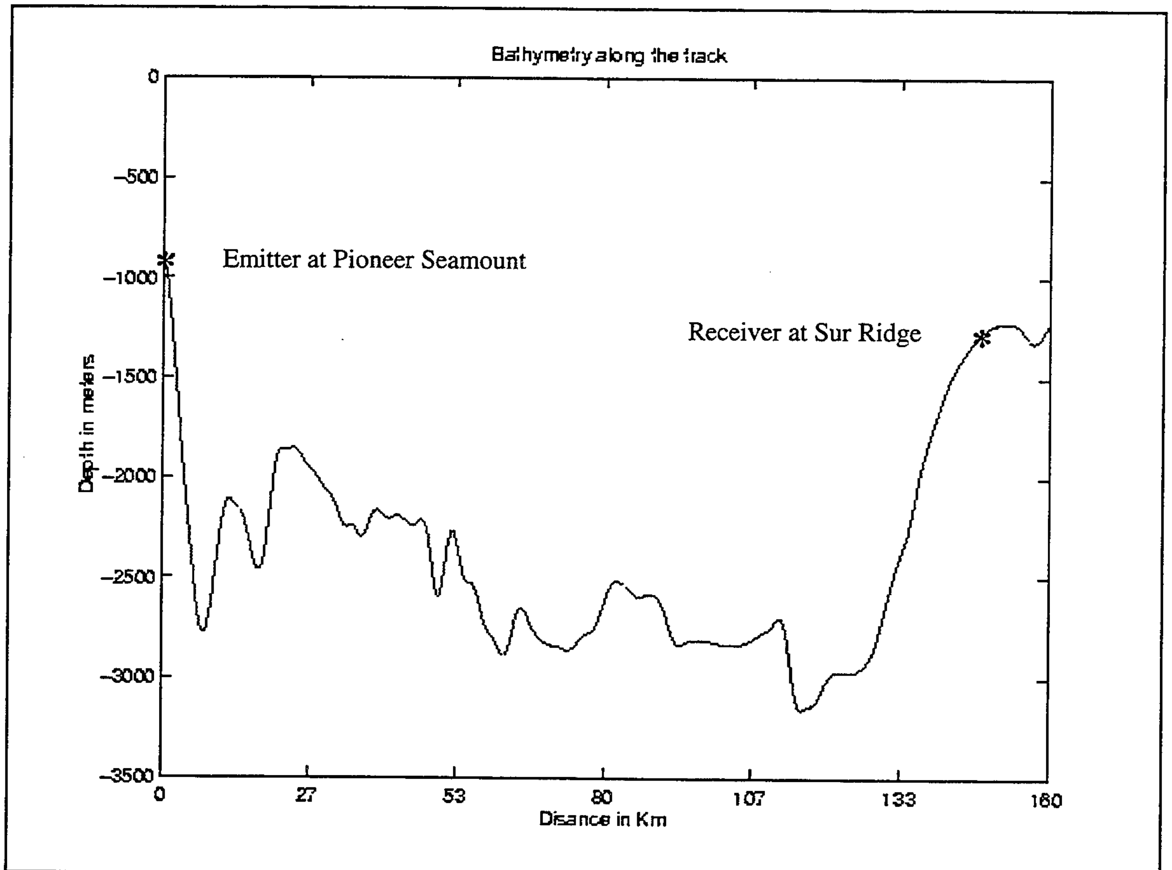

Figure 2. Bathymetry between Pioneer Seamount and Sur Ridge

The transmitter is located on Pioneer Seamount (Fig. 1) at a depth of 940 m. This Alliant Techsystems HX554 acoustic source produces a 260 Watt, 75 Hz phase modulated signal. An underwater cable connects the sound source to a shore facility at Pillar Point where the ATOC equipment shelter controls the state, period and power of the transmitter and the transmission schedule (Howe, 1996).

The NPS OAO receiver is located south of the Pt. Sur Light House. It records unclassified data from a single hydrophone of a former US Navy surveillance undersea hydrophone array located on Sur Ridge. The hydrophone lies on the bottom at a depth of 1320 m (see Fig. 2).

The bottom bathymetry between transmitter and receiver is interpolated from a 250 meter resolution bathymety data set covering the Monterey bay area (U. S. G.S., Menlo Park, California). The locations of the transmitter and receiver are well within the geographical limits of this data set. A difficulty was to place the transmitter and receiver at the right spot in this data base. Due to the tormented aspect of the bathymetry along the pass, iterative analyses to fine-tune the geographical locations of the source and receiver were needed to match the acoustic model output to the observations.

2. Sound transmission recording

Data collection began on 10 April 1996 and continued through 20 February 1997.

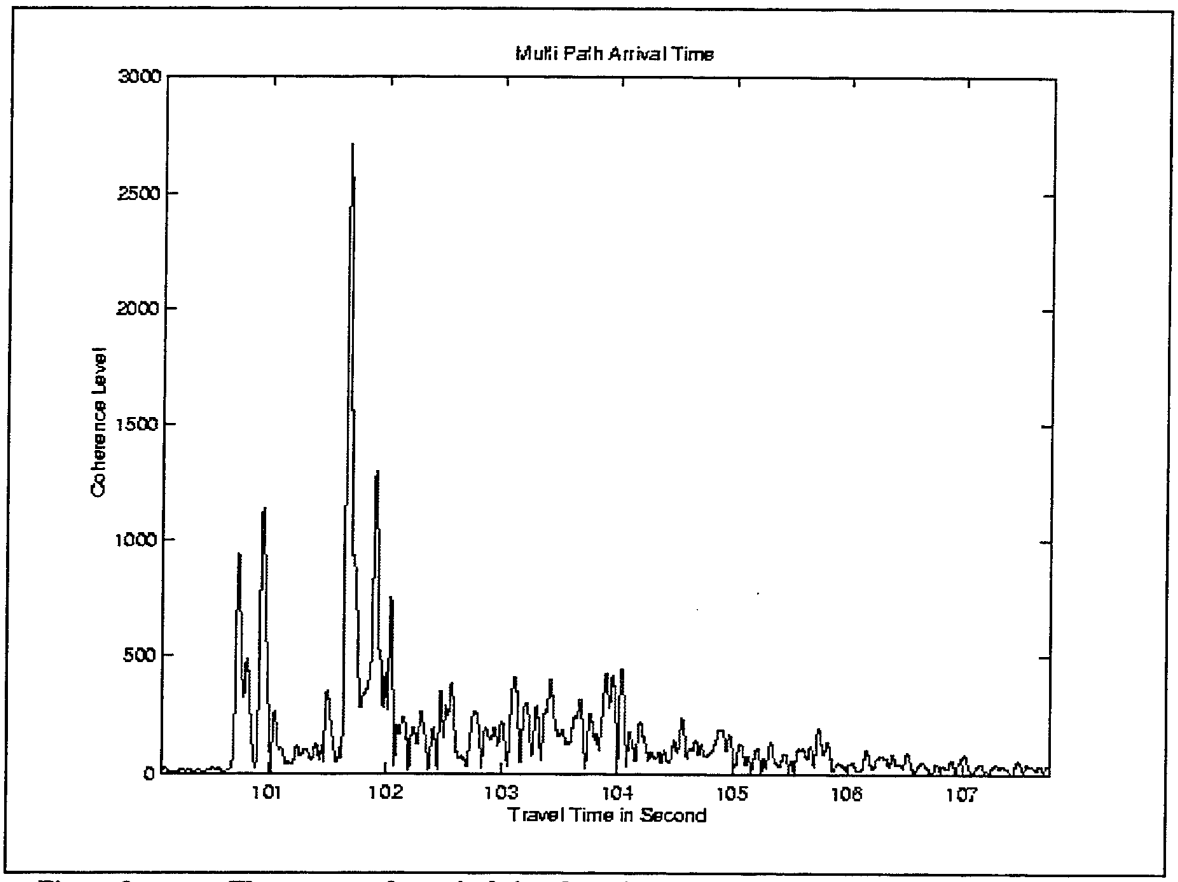

Figure 3. The pattern of a typical signal received at Sur Ridge showing multipaths, strong peaks and a high signal to noise ratio.

After 20 February, the transmitter was disabled due to a cable fault caused by fishing activity. During the data collection period, a total of 429 phase modulated transmissions were received at the OAO. Global Positioning System (G.P.S.) provided the timing synchronization between the transmitter and receiver, both fixed to the sea bottom. Stored at NPS, all the sound tracks were processed with a correlation matched filter. The output corresponds to a sum of pulses, arriving from the multiple eigenray paths (Fig. 3). Each pulse has a duration of 27.28 ms.

3. Arrival Structure

Extracting the maxima that exceed a threshold from all the coherence curves enables us to generate a dot plot of the eigenray travel times. The dot plot is shown in Fig. 4 displaying repeated peaks of stable arrivals from transmission to transmission. This map of peaks enables us to see the different individual rays and ray groups at the

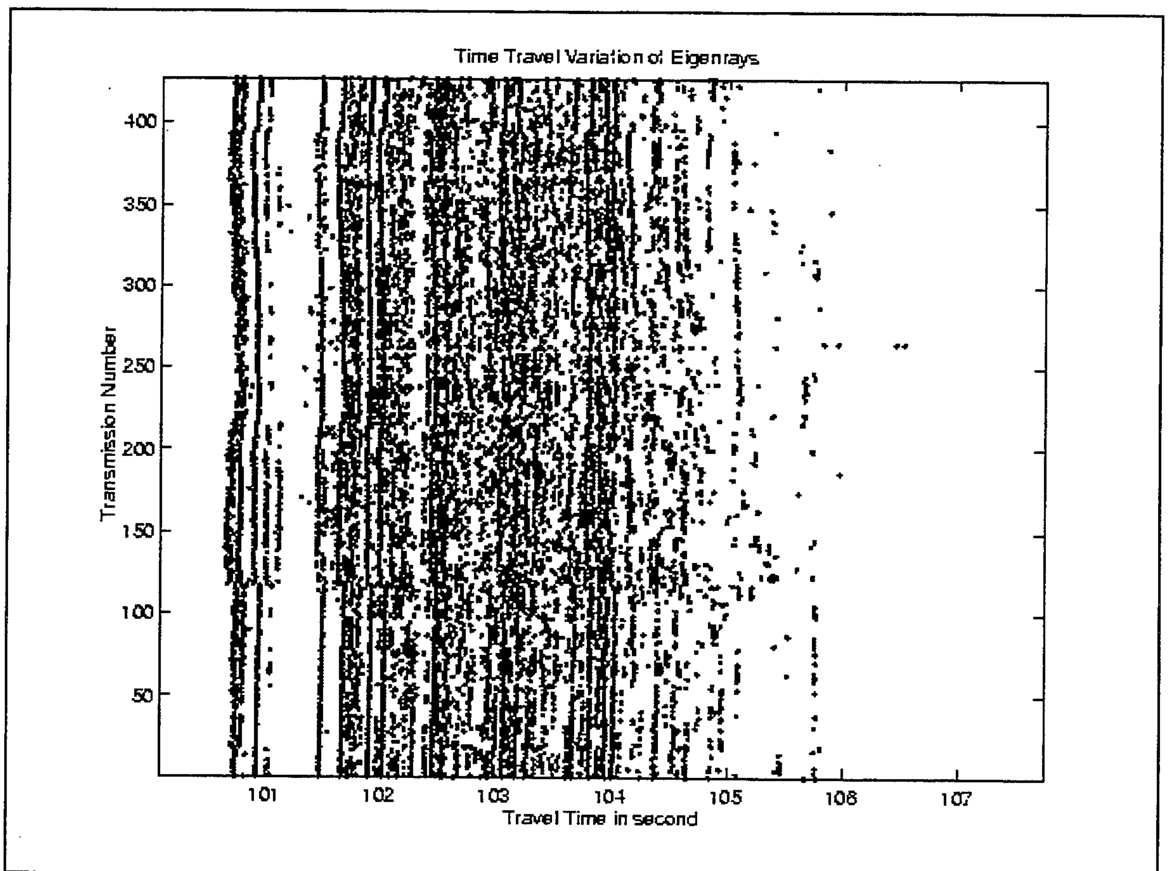

Figure 4. Dot plot of strong peaks in the arrival pattern of each of each of the transmissions. The aligned dots indicate stable arrivals over the duration of the experiment.

receiver location. The variations of the ray travel time are seen to be small around the means. The observed acoustic stability, repeatability and small perturbations from the mean are crucial to the applicability of acoustic tomography.

The dot plot also shows jumps over some parts of the repeated transmissions. These jumps are due to the intermittence of the transmission schedule which presented long gaps of fifteen days to one month. These gaps introduced slight difficulties in the time series extraction process and also in the inverse tomographic analysis and will be discuss later on.

B. HYDROGRAPHIC OBSERVATIONS

1. "Point Sur" Summer Cruise

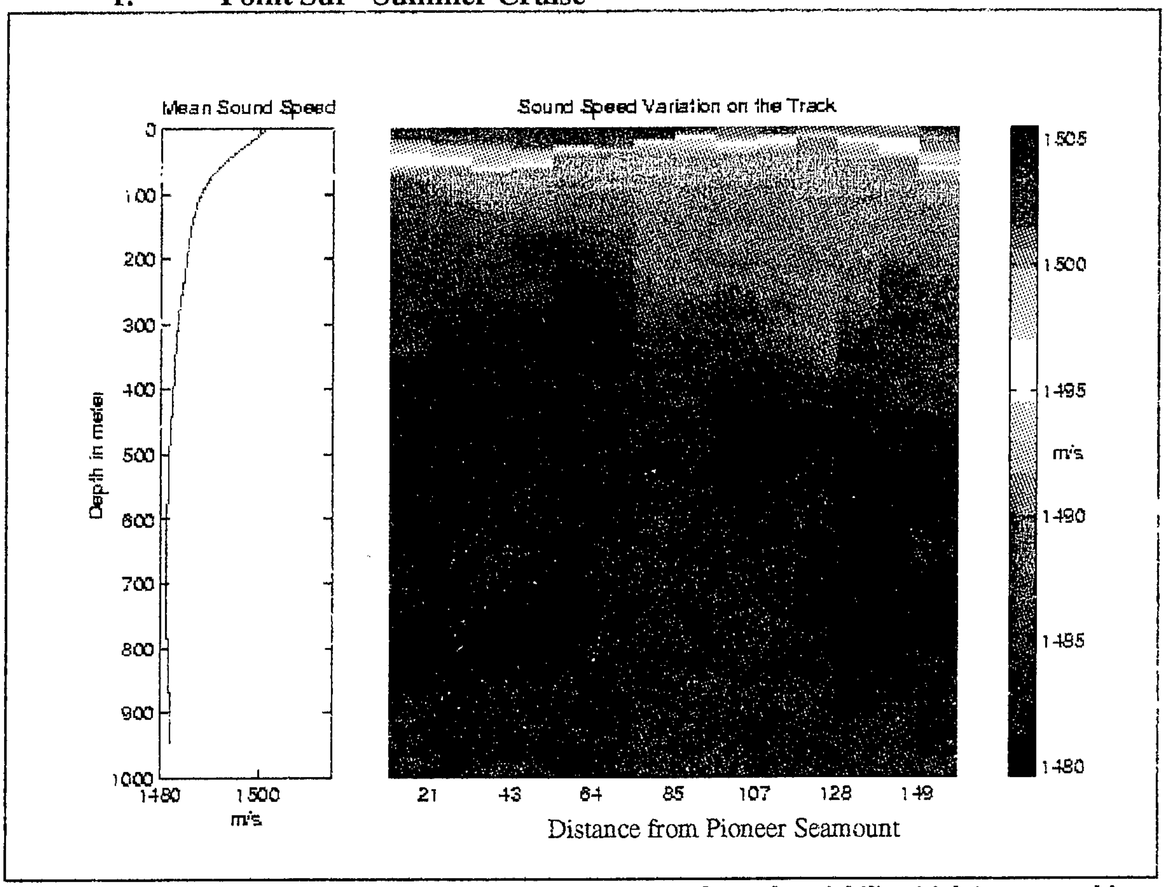

Figure 5. Mean sound speed profile (left) and sound speed variability (right) measured by Point-Sur ship survey consisting of 14 CTD stations between Pioneer Seamount and Sur Ridge.

In July 1996 a cruise was conducted between Pioneer Seamount and Sur Ridge to collect CTD data to initialize our acoustic modeling (Collins et al., 1997).

Fourteen CTD stations were occupied and the data are displayed in Fig. 5 in terms of sound speed.

A mean, filtered profile without fine structure was estimated from the CTD casts. This mean profile (shown in Fig. 5) was used to represent the "background" or "reference" ocean in the "forward" and inverse tomographic analyses. Note that the deep sound channel is at about 700 m so both the transmitter and receiver are below it and there is no shallow sound channel.

2. The Monterey Bay Aquarium Research Institute (MBARI) Mooring

The MBARI moorings M1 and M2 collected ocean temperature and wind data that are important to this study. They provided at different steps vital information for the

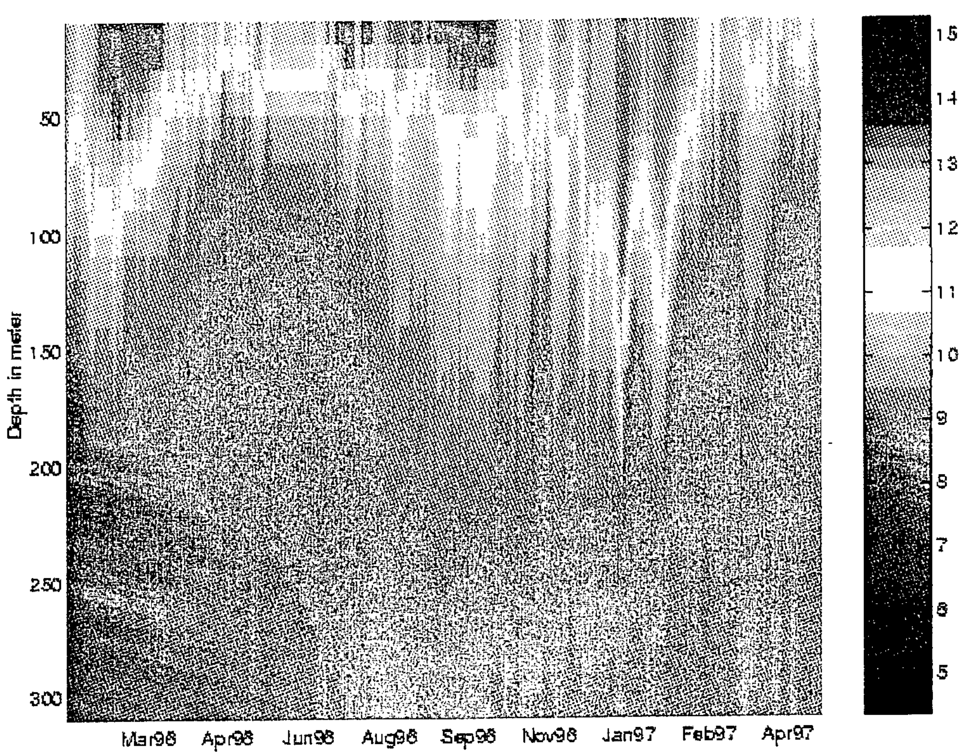

Figure 6. Temperature variation at MBARI mooring.

constraining, verifying and analyzing of the tomographic estimate. The MBARI moorings M1 and M2 (see Fig. 1) are not on the acoustic track. M2 is nearer but was not working during the time period of the tomographic transmissions. Despite this, the M1 mooring has enabled us to correlate the tomographic estimate to the direct temperature and wind observations. Data from M1 was also used to provide an EOF constraint to improve the tomographic estimate.

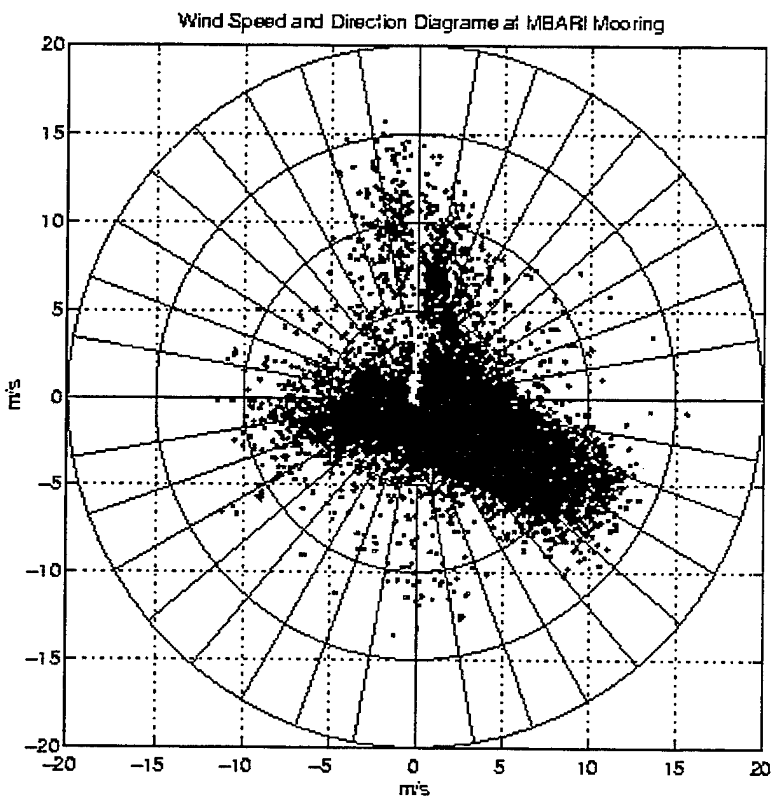

Figure 7. **Scatter plot of wind speed and direction measured at MBARI mooring M1 showing NW and SSE winds distribution.**

The wind speed and direction between January 96 and April 1997 at the MBARI M1 mooring show dominant NW winds (see Fig 7). Those winds were directly responsible for the upwelling occurring along the California Coast. We also see several strong SSE wind events around December 1996 (see Fig. 8) which correlate well with downwelling of warm water as observed in the temperature record shown in Fig. 6. After replacement, MBARI mooring M2 allowed us to verify the hypothesis made on the spatial extension of an EOF to the acoustic track.

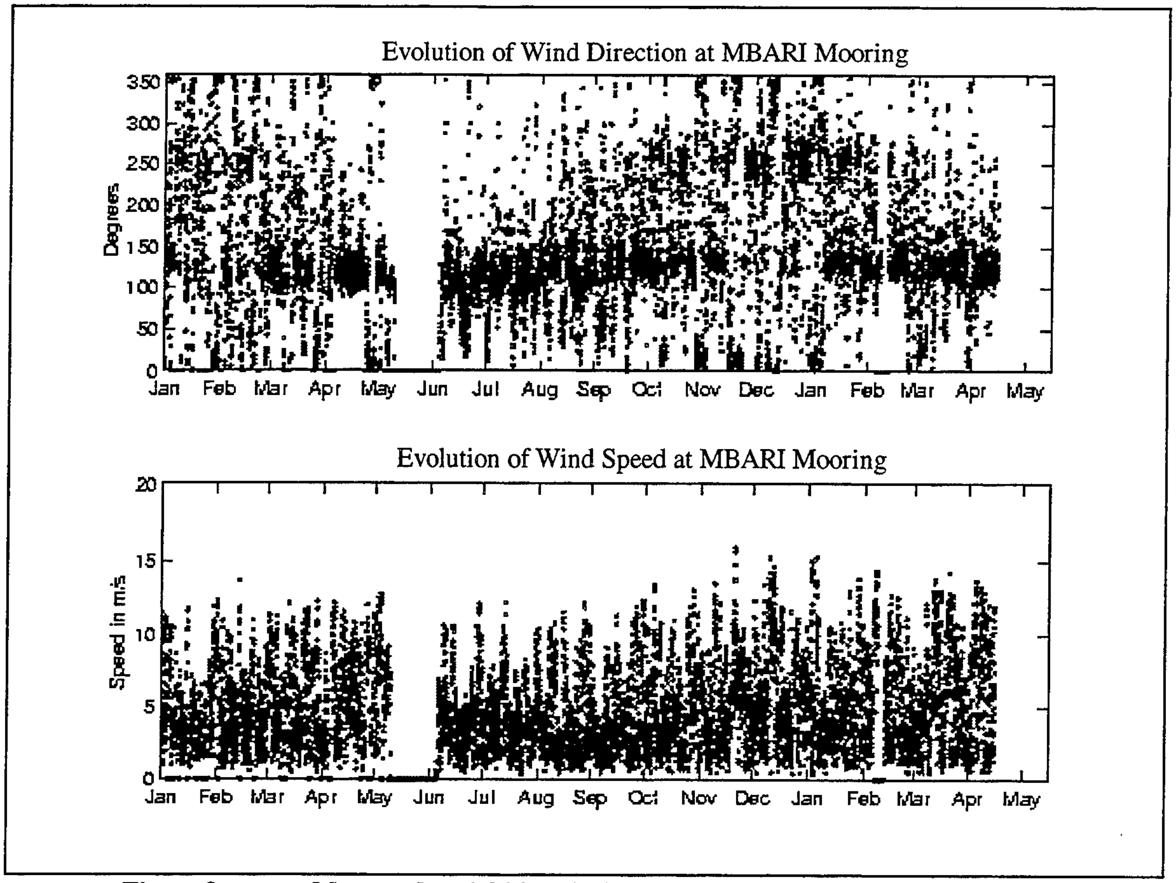

Figure 8. **Measured variability of wind direction and speed at the M1 Site.**

III. TOMOGRAPHY FORWARD MODELING

A. PROPAGATION MODELING

Modeling the received signal is a required step in solving the forward problem of ocean acoustic tomography. Ray identification and path association, key to establishing the data set of travel-time changes and the mathematical relations between the data and the unknown sound-speed perturbations, are achieved by comparing the modeled signal to the observed signal.

Sound travels through the ocean following different paths from the transmitter to the receiver which are called eigenrays. At the receiver, the pressure disturbances associated with the different eigenrays have different time delays, magnitudes and phase shifts. These multipath pressure disturbances add up to give a complex pattern that has an extended time duration. In mathematical terms, the received signal (i.e., arrival structure) can be expressed as:

$$\tilde{r}(t) = \sum a_n \tilde{S}\,(t - t_n)\, e^{-i\,(2\pi f_o t_n + \phi_n)}$$

where $\tilde{r}(t)$ is the complex envelope of the received signal, $\tilde{S}(t)$ is the complex envelope of the emitted signal, f0 is the carrier frequency of the transmission, and t_n, a_n, ϕ_n are the time delay, magnitude modification and phase shift, respectively. Thus, modeling the arrival structure requires tracing the raypaths, searching for eigenrays, and determining t_n, a_n, ϕ_n.

Tracing the raypaths was accomplished using an upgraded version (Chiu et al., 1994a) of the Hamiltonian Acoustic Raytracing Program for the Ocean (HARPO) (Jones et al., 1986). Input to HARPO was the mean sound speed profile from the CTD cruise and the Pioneer-to-Sur Ridge bathymetry extracted from the 250-m-resolution data set, which collectively define the "reference state" of the ocean. A fan of rays was launched with initial elevation angles from -30 to + 30 degrees with an increment of 0.001 degrees. The output of HARPO includes the geometry of the raypaths and the travel times. For the simulation of the arrival structure, a computer program developed by Chiu (1995) called "ray3d" was used to operate on the output of HARPO. This program searches for eigenrays, calculates the travel times to the receiver, counts and keeps track of the phase shifts caused by turning points and bottom and surface reflections, and estimates signal level reductions due to raytube spreading and bottom and surface bounces. Given the envelope of the source signal, the program then computes the envelope of the received signal according to the above equation.

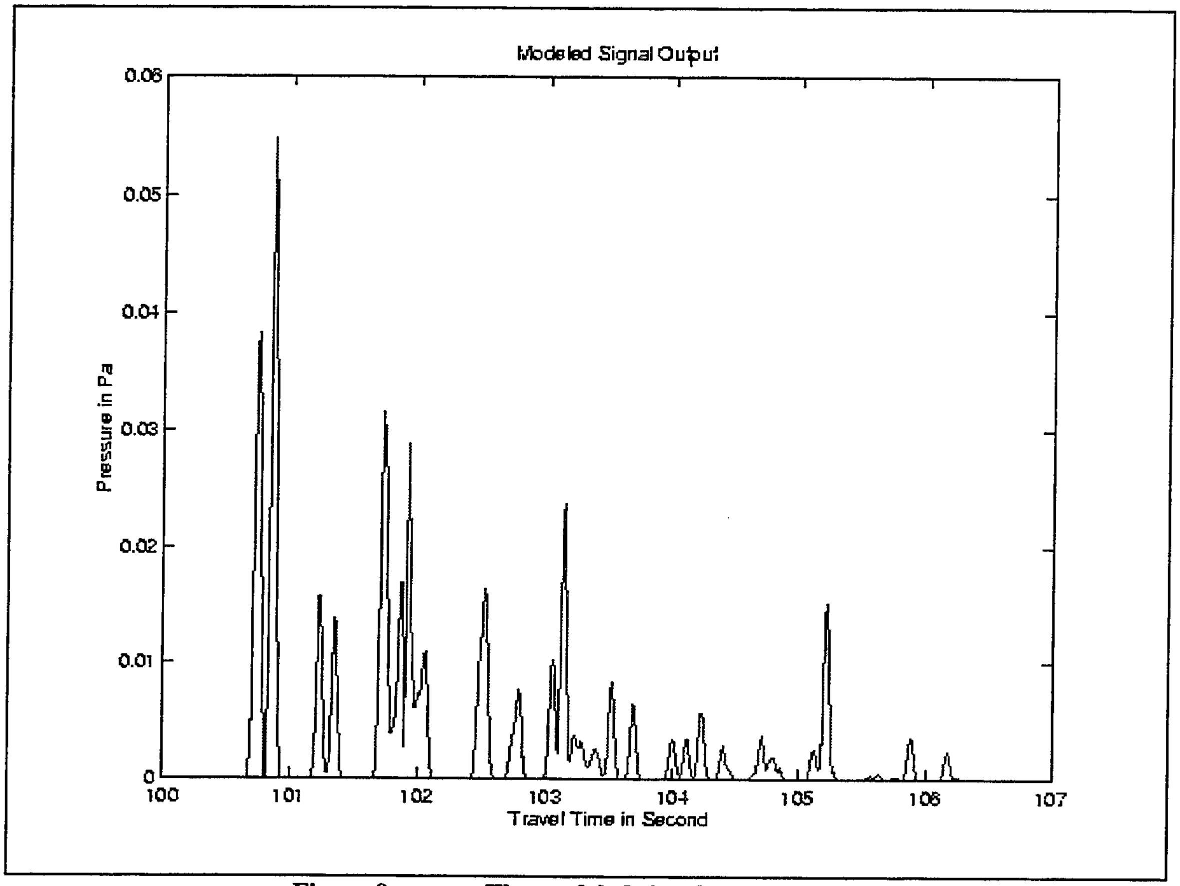

Figure 9. The modeled signal arrival pattern

The modeled arrival pattern is shown in Fig. 9. A visual comparison of the modeled and observed patterns (shown in Fig. 3) show that the gross structure is similar. A detailed comparison between the predicted eigenray arrivals and the observed peaks will be presented in the next chapter. A total of 106 eigenrays with varying magnitudes, phase shifts and travel times in this 60-degree ray fan was obtained. In Fig. 10, a ray diagram showing some of the eigenrays connecting the transmitter and receiver is also displayed along with the bathymetry. Constructing the envelope enables us to compare the theoretical signals with the real one. If the two structures match, then we can proceed to identify the observed arrivals structure to the modeled eigenrays.

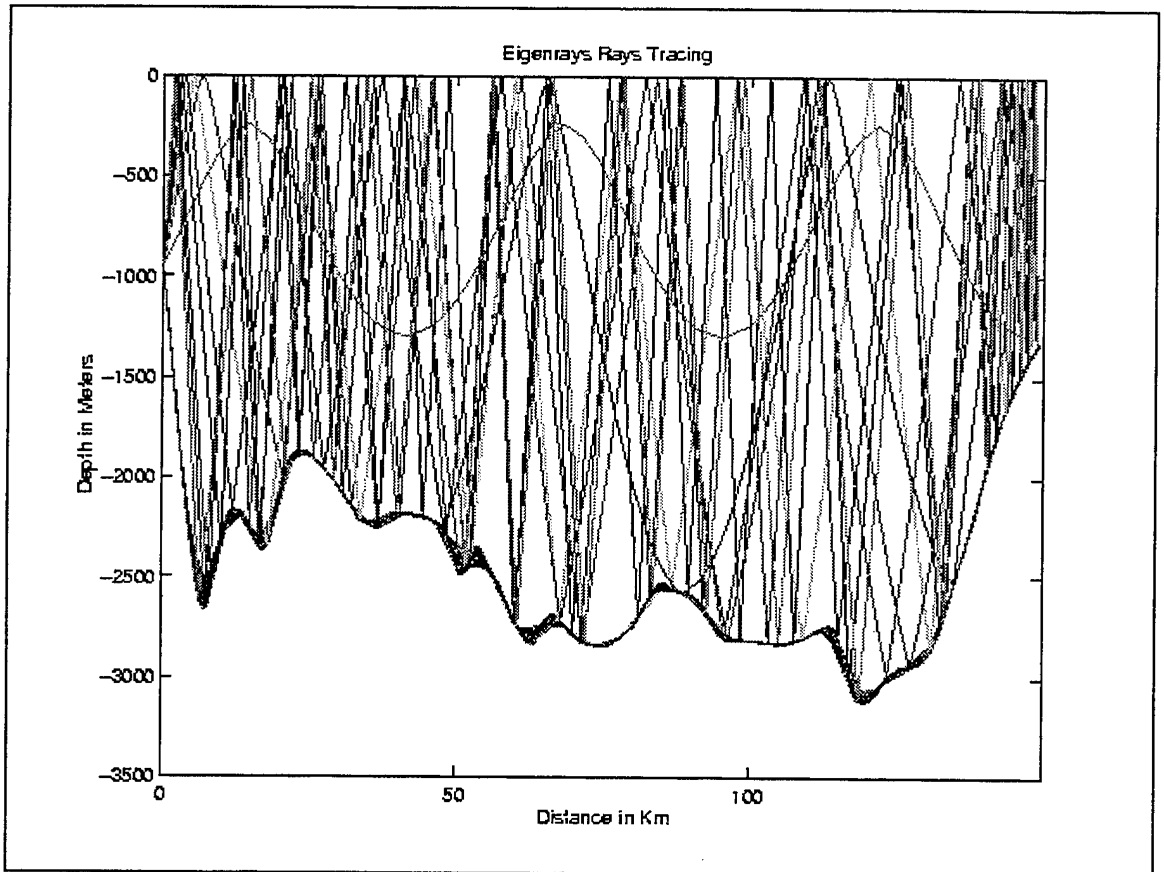

Figure 10. The geometry of some of the Eigenrays.

The forward modeling is a very important step toward the solution of the tomography inverse problem. It enables us to develop the association between a travel time series and an eigenray provided by the model.

B. CONSTRUCTION OF TRAVEL TIME DATA SERIES

The extraction of the data series of travel times for different arrivals was not fully automated. The problem is that the transmissions have large time gaps and the travel time

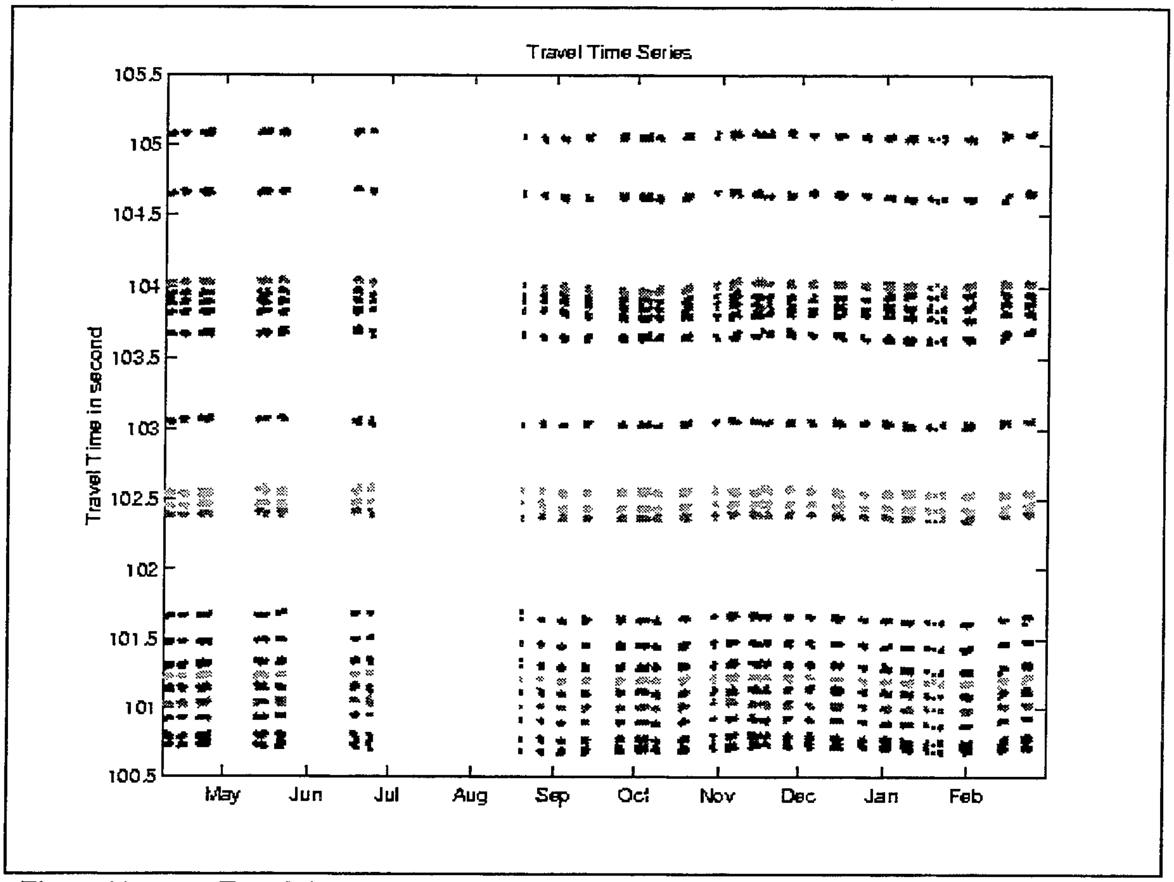

Figure 11. Travel time series showing transmission gaps over the duration of the experiment.

of an individual arrival can change more than the separation between individual arrivals over those large gaps. To deal with the problem computer program that interfaces with a human operator was developed. This program extracts the travel time of a peak in a window. The window moves in geophysical time (i.e., day, month, year) with its center following a piecewise linear curve defined by the operator, based on a threshold map of all the peaks. Twenty high quality time series extracted from this semi-automatic procedure are shown in Figure 11.

C. TRAVEL TIME VARIABILITY

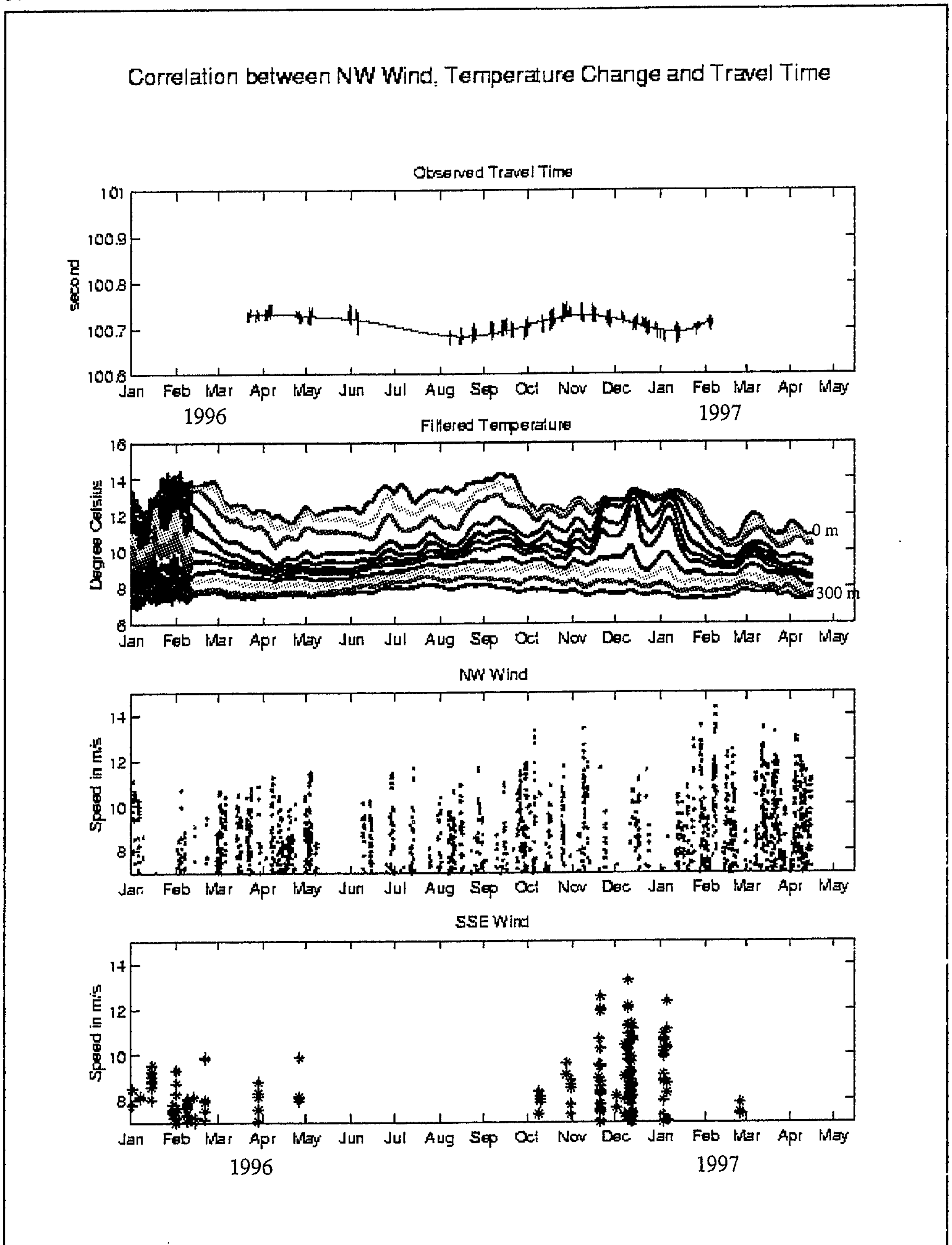

Figure 12. Observed variability: (one) in the travel time of one of the ray arrivals, in the data recorded at MBARI mooring; (two)temperature records M1, first part of the graph shows the daily variation; (three) in the NW wind speed linked to upwelling and (four) SSE wind speed linked to downwelling.

Figure 12 shows, respectively, the variability in the travel time of an arrival eigenray, and the observed MBARI mooring temperature and wind data. This figure is used next for a discussion of the relationship between the observed changes in the displayed environmental variables.

1. Diurnal variation

In all the travel time series, diurnal variations were observed that were also present in the near-surface temperature time series measured by the MBARI M1 mooring (unfiltered part of sub-plot 2). These variations were expected to be mostly due to the fluctuation of the mixed layer depth. All the eigenrays are affected by this diurnal effect because they are either reflecting at the surface or have shallow upper turning point depths. Thus they all sample the variability in the surface layer.

2. Synoptic scale events: downwelling

Between December 1996 and March 1997, two downwelling events are captured by the moored temperature records which appear to be induced by strong SSE winds. They appear as a travel time decrease due to the overall increase in temperature/sound speed.

3. Seasonal evolution

A seasonal oscillation is clearly shown in the travel time data. This oscillation come from evolution of the mixed layer depth over a large area caused by seasonal wind and solar insolation. This oscillation is clear in the moored temperature data at the M1 site. The increasing travel time from April through June 1996 and in February 1997 were linked to the upwelling events due to NW winds blowing strongly during those two periods. Due to the cooling of the upper ocean from below by the upwelling, the temperature lines converge towards the deep one, the sound-speed decreases and thus the travel time increases. Unfortunately, the transmitter failed before the beginning of March 1997 which deprives us of examining the travel-time signature of the 1997 El Nino event.

4. Inter seasonal variability

For the eleven month travel time series we can see from April 1996 to early February 1997 a slight negative trend in the travel time. This implies an annual heating along the 160 km track between Pioneer Mountain and Sur Ridge. Was that trend a "preamble" to an El Nino event? Further observations and data analysis will be needed to answer this question.

IV. TOMOGRAPHIC INVERSE ANALYSIS

A. VERTICAL STRUCTURE AND CONSTRAINT

There is lack of vertical resolution in the tomographic observations. The depths of emitter and receiver are not optimum. Both are lying on the sea bottom far below the axis of the deep sound channel. As a result, all the eigenrays are either surface reflecting or have very shallow upper turning points resulting in mostly redundant information on the vertical ocean structure. Nevertheless, this lack of vertical resolution does not severely affect the quality of the tomographic estimate because the ocean under investigation was dominated by a single vertical mode, that is, the ocean itself has a smooth vertical structure. This characteristic of the ocean vertical structure can be demonstrated using the temperature records from the MBARI moorings in conjunction with an empirical orthogonal mode (EOF) analysis. The dominant EOF was, in turn, used to constrain the tomographic estimate resolving the horizontal and temporal structure of the temperature field.

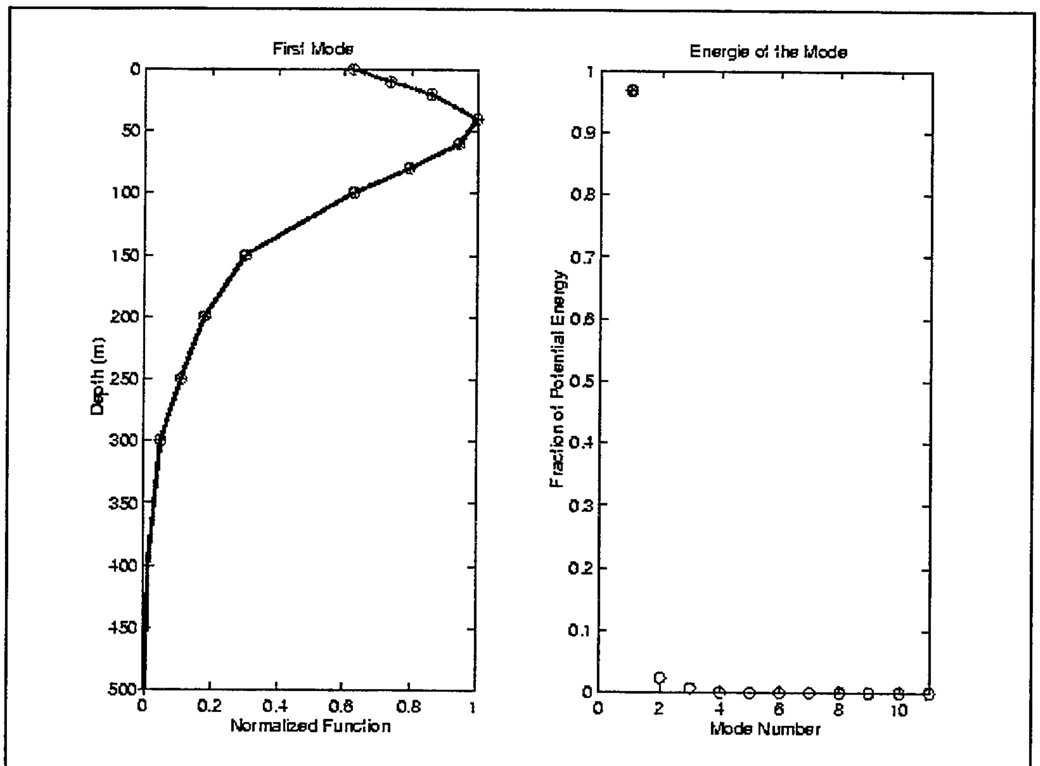

Figure 13. First vertical mode (left) and distribution of modal energy (right) derived from an EOF analysis of the depth records of ocean temperature measured at the M1 site.

The temperature records were first filled using a low order polynomial. For the M1 mooring, hourly temperature data at 11 depths spanning the first 300 m were obtained. The main results from the EOF analysis of the M1 data are:

- The first mode contains 98% of the potential energy and has a maximum at 40 m (see Fig. 13).
- The second mode, which was analyzed, is a surface intensified mode with energy mostly confined in the first 20m of the water column. It however contains only 2% of the total potential energy.

The results from the EOF analysis of the M2 data are similar. The M2 results will be discussed in a later section.

- In constraining the vertical structure of the tomographic estimate, a curve was fitted through the first EOF assuming that the mode goes to zero in the lower ocean. This mode, extrapolated to great depths, is shown in Figure 13 and it was assumed to be geographically independent along the coast over the whole tomographic transmission path.

B. RAY IDENTIFICATION AND DATA TREATMENT

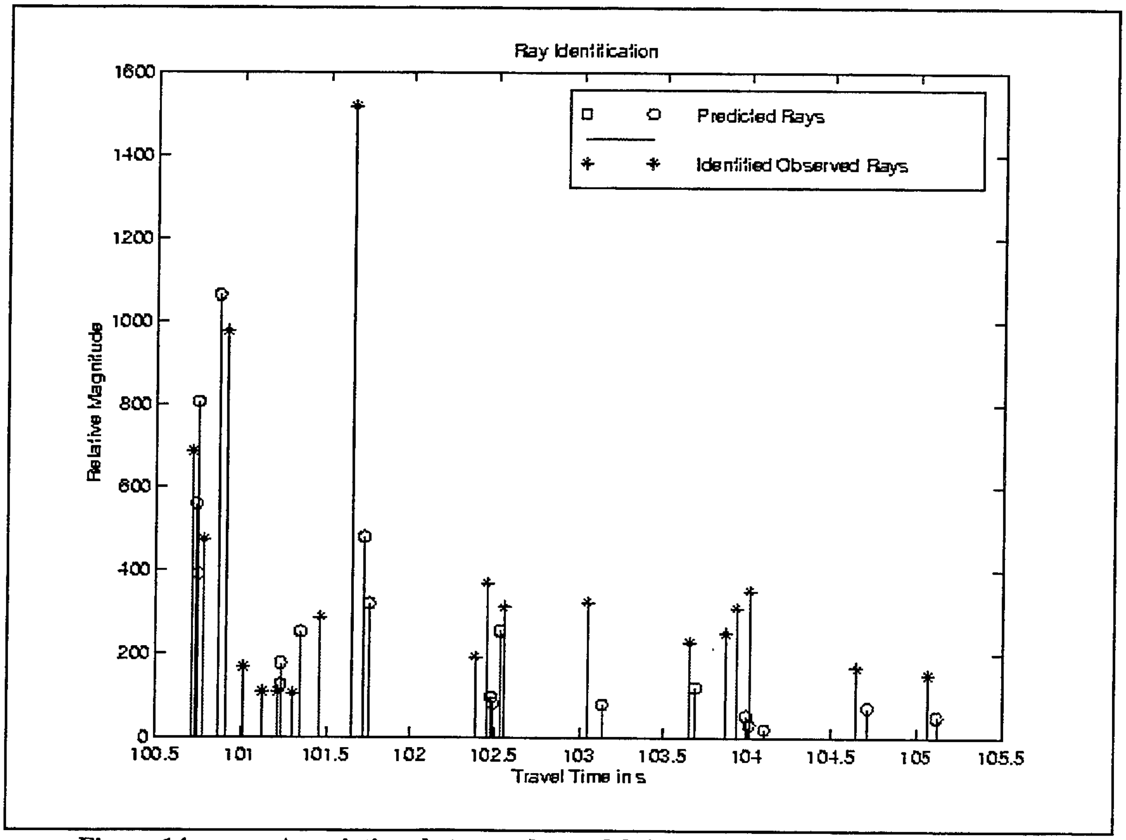

Figure 14. Associations between the modeled eigenrays and the observed mean magnitudes and travel time of the significant arrival peaks.

Ray identification is an important part of a tomographic analysis. It assigns the observed travel time data to the modeled eigenrays in the reference ocean. This was accomplished by comparing the observed mean arrival structure to the predicted arrival structure (Fig 14.). Since we were dealing with quasi-resolved individual rays, a time window of 0.03 seconds, centered at the mean arrival time of each extracted time series, was used to guide the assignment. The strongest of the eigenrays in the window was selected and a total of nineteen eigenrays was picked.

Due to the intermittence of the acoustic emission, the gaps in the data series of travel time were filled using an eighth order least-squares polynomial curve. Polynomials of orders above eight had a tendency to over shoot in the large gaps. An eighteen-day lowpass filter was then applied to the time series to eliminate the daily variations which were not the subject of this investigation.

C. INVERSE SOLUTION AND TOMOGRAPHIC RESOLUTION

Based on the predicted raypath geometry and integral relation between travel time and sound-speed perturbations, the 19 data series of travel times were "inverted" using a standard procedure. A detailed outline of the method can be found in Chiu et al. (1994 a). In short, the method is based on a Fourier decomposition of the sound speed perturbations and a minimization of an objective function. With specified noise variance, solution variance and ocean decorrelation scales, it constructs an optimal estimate of the Fourier coefficients that has minimum mean square errors. Additionally, it produces system resolution and solution error estimates, and using multi-dimensional Fourier transforms, the inverse solution and its error and resolution measures are transformed from the spectral space back to the physical space.

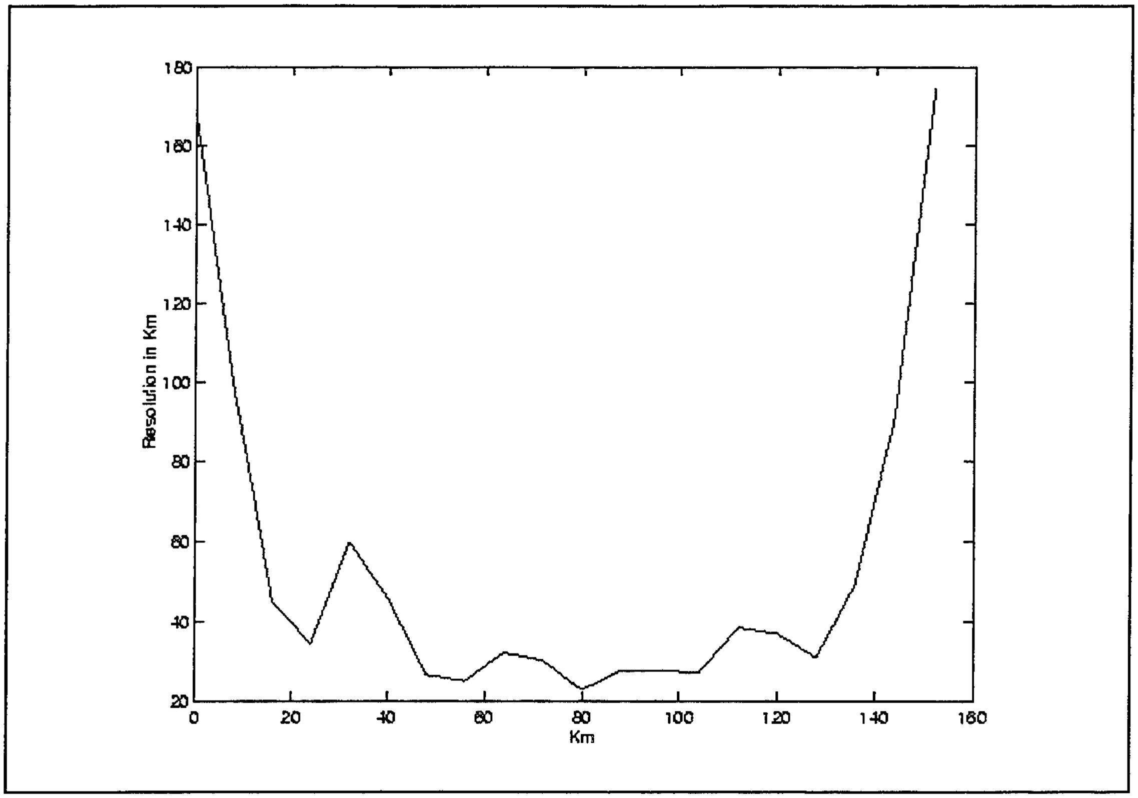

Figure 15. Horizontal resolution length of the tomographic observations on the transmission path from Pioneer Seamount to Sur Ridge.

In this analysis, an iterative solution was used to refine the *a priori* statistical information until the statistics of the final solution and data residual were consistent with the assumed values for the statistical parameters. The horizontal variation of sound speed was decomposed into 20 Fourier components, equivalent to discretizing the perturbations along the160-km horizontal distance between Pioneer Seamount and Sur Ridge at an increment of 8 km in physical space. The vertical structure was fixed with the first EOF. At each iteration, the inverse method processed the travel time records to give daily estimates of sound-speed perturbation over a period of 11 months. In the final iteration, the input statistical parameters assumed the following values: 225 m^2/s^2 for the solution variance, 16 ms^2 for the noise variance, and 24 km for the horizontal ocean decorrelation length.

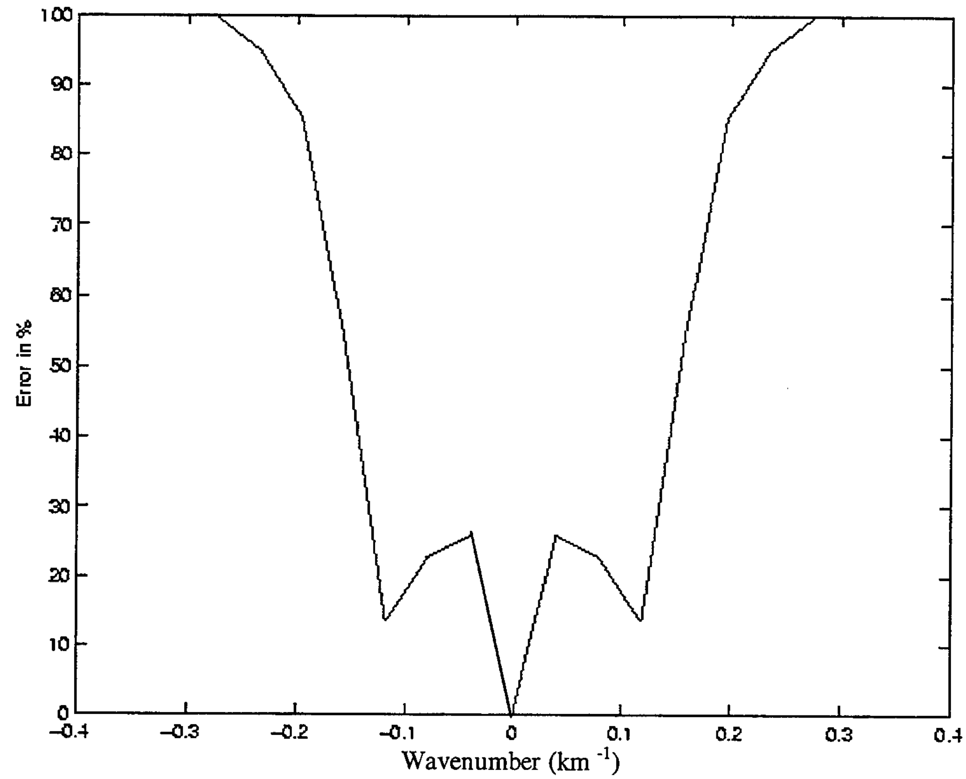

Figure 16. Error distribution in the Fourier domain of the tomographic estimate.

The horizontal resolution of the tomographic estimate is illustrated in two separate but equivalent figures. Fig. 15 shows the minimum resolution lengths along the transmission path in physical space, revealing an average resolution of about 30 km, excluding locations near the emitter and receiver where the density of raypath crossings are minimal. Fig. 16 shows the error in the tomographic solution in the Fourier domain. It indicates that spatial variations with wave-numbers bounded between -0.2 and +0.2 km^{-1} (or wavelengths of 30 km and longer) were adequately resolved. It also indicates that the evolution of the spatial average was accurately determined, due to the integrating nature of the data.

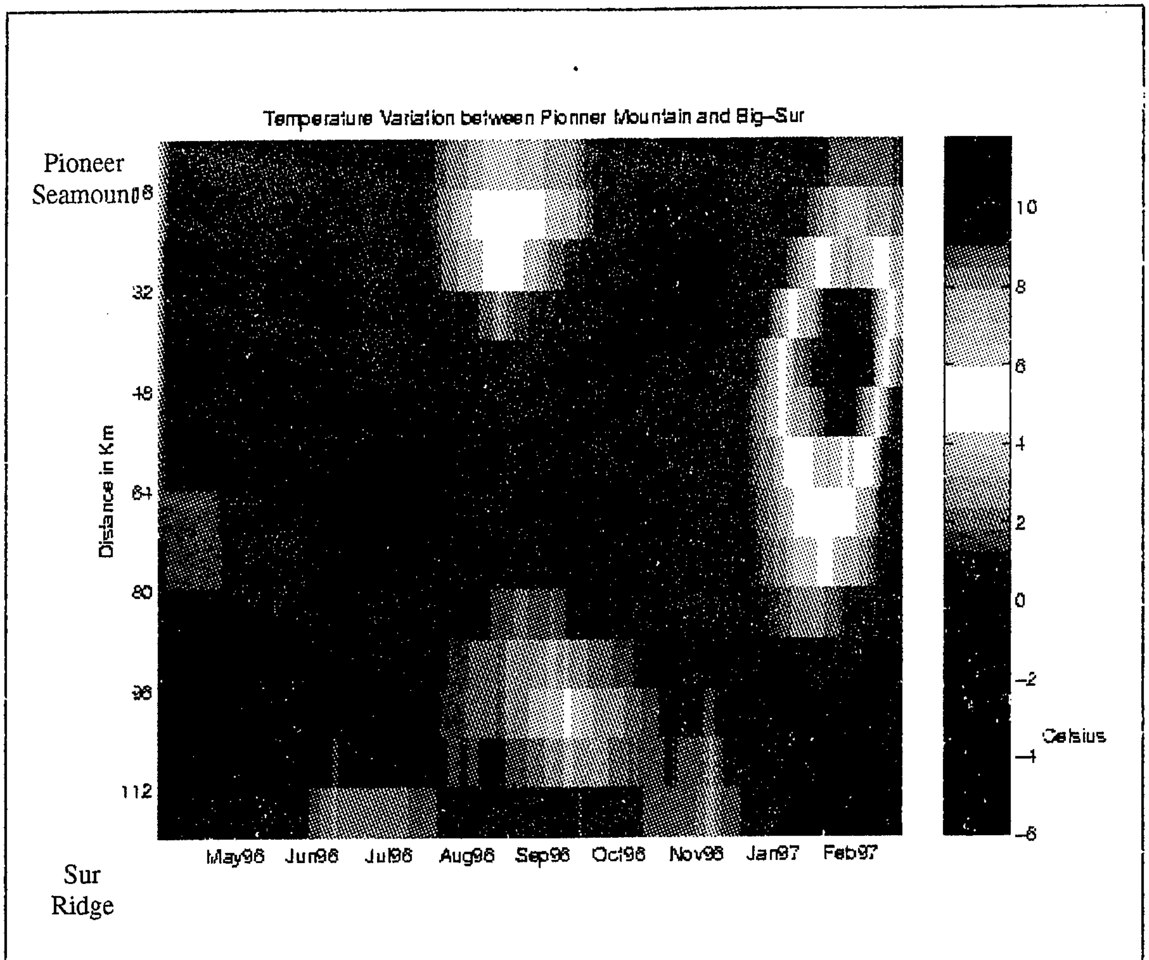

Figure 17. Temperature variability at 45 m depth between Pioneer Seamount and Sur Ridge

The tomographic inverse solution for sound speed, converted to temperature perturbation, is shown in Fig. 17. Only the temperature variation at a depth of 45 m (where the EOF reaches a maximum) as a function of horizontal distance and geophysical time is displayed. It is seen that tomography observes overall cooling from April to July and in November 1996, and mild warming during summer time. It is also detects an exceptional increase in temperature in the northern half of the transmission path in January and February 1997. During this winter period and in this northern half, tomography measured an increase of 7 to 8 degrees Celsius at a depth of 45 m. An explanation of this unusual winter time temperature increase will be given following a validation of the tomographic results using the moored temperature data.

D. VERIFICATION

As most of the energy is trapped in the first 300 m, it makes sense to check the quality of the tomographic estimate by comparing the layer average of the estimate to the depth-averaged M1 temperature data. The temporal evolution of the layer-averaged tomographic estimate and the depth average M1 temperatures are displayed in Fig. 18 and shows good agreement in amplitude and phase. The small differences are normal as the travel time data series were low-pass filtered in time and the inverse solution was also averaged in distance. Additionally, tomographic and M1 sampled a non-over-lapped location.

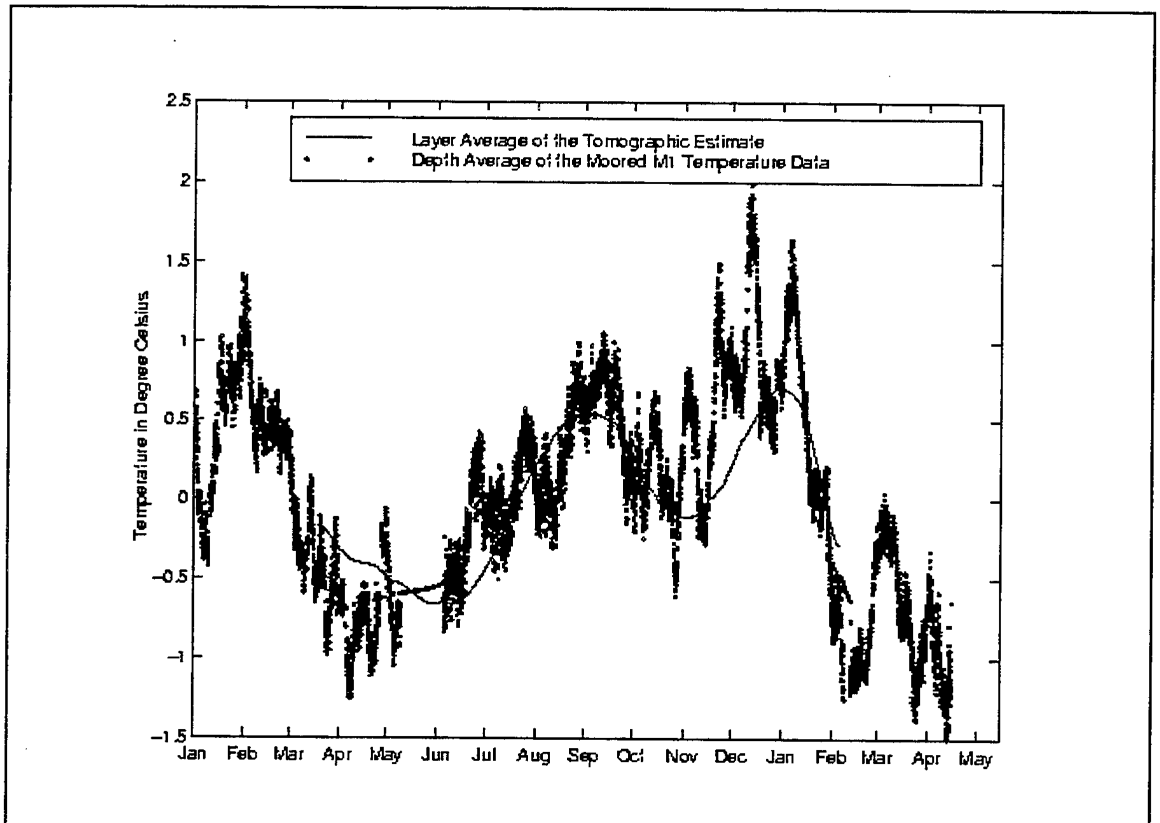

Figure 18. Comparison between the layer average tomographic solution and the depth-averaged mooring temperature data at M1.

In obtaining the tomographic solution, the first EOF derived from the M1 mooring was imposed as a constraint. To check the adequacy of this assumption, an EOF analysis was also performed on the temperature record from M2 which is closer to the acoustic path. Since M2 had no data covering the same period of tomographic transmissions, data from 1997 were analyzed instead. The EOF analysis of the M2 data indicated similar results (see Fig. 19) confirming the extendibility of this simple-dominant mode hypothesis.

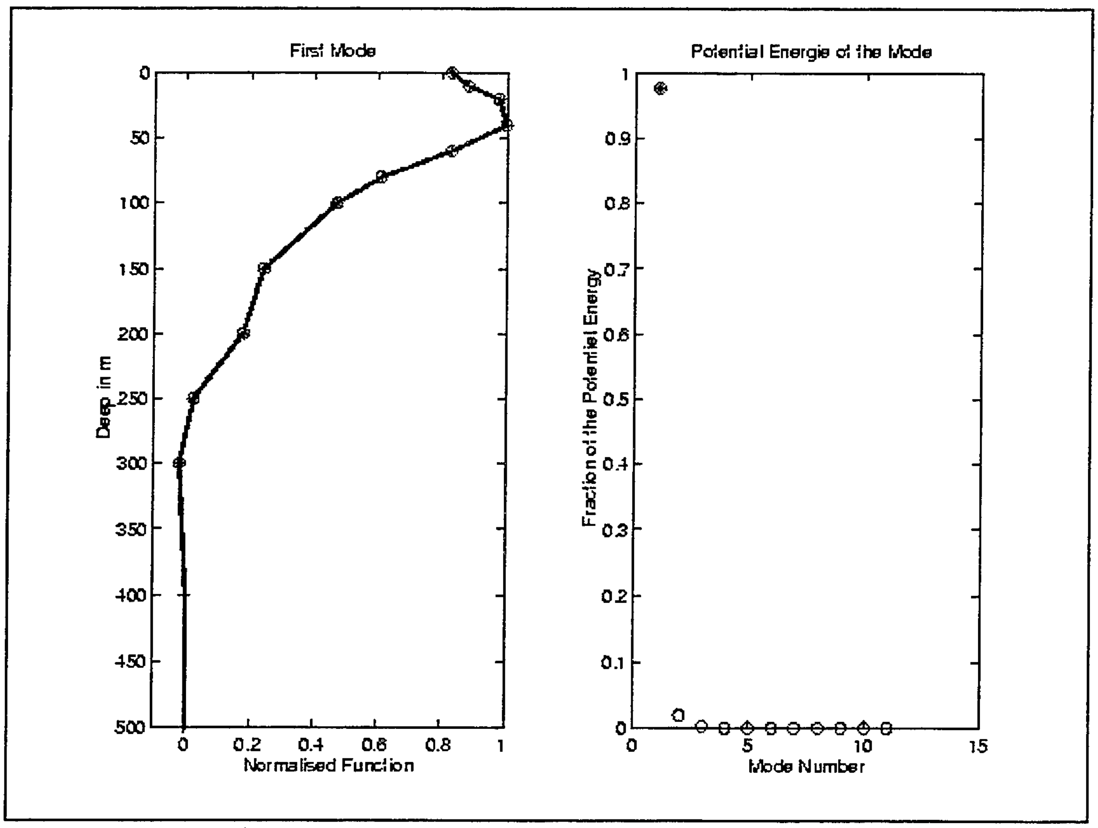

Figure 19. Vertical structure derived from MBARI M2 mooring.

E. INTERPRETATION OF OBSERVED TEMPORAL AND SPATIAL VARIABILITY

The complementary data from MBARI M1 mooring was used to facilitate an interpretation of the different events taking place along acoustic path as seen in the tomographic solution. Such an interpretation can enhance our knowledge of the relations between the tomographic observations and the upwelling and downwelling coastal

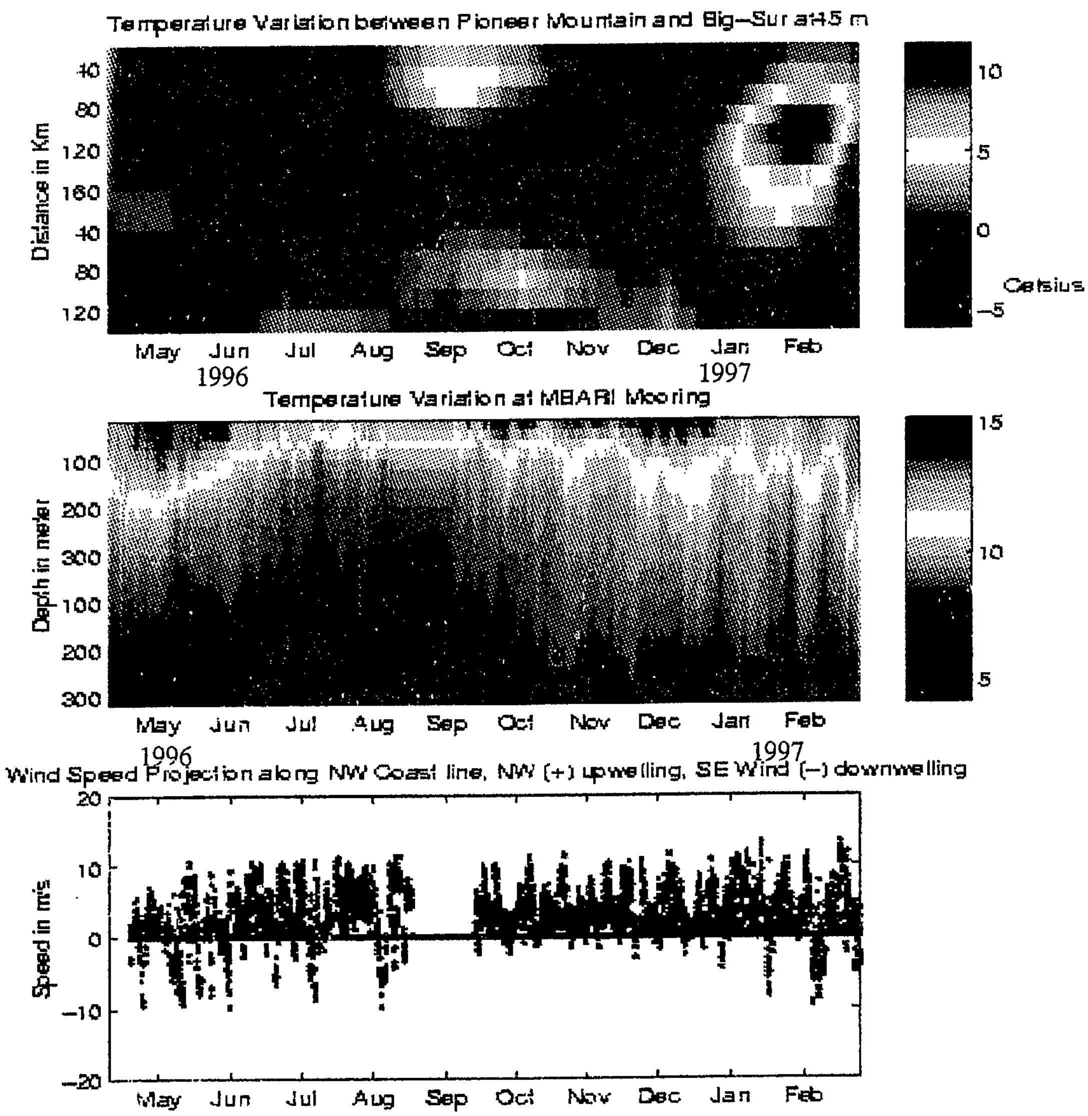

Figure 20. Variability in the tomographic estimate (top), in the M1 temperature data (middle) and on the M1 wind observations projected along NW coast line.

processes. The tomographic estimate is displayed in Fig. 20 together with the M1 mooring temperature records and the M1 mooring wind speed projected along NW oriented coast line (see Fig. 1), NW wind component positive linked to upwelling, SE wind component negative linked to downwelling.

From January to the end of February 1997, alternative SE and NE winds were observed giving synoptic-scale warming signatures in the MBARI temperature record that coincide with a large warm spot in the inverse tomographic solution.

These warming signatures only appear in the middle of the northern part of the tomographic path but not in the southern half. An explanation is that the middle of the northern half is the closest point to the shore and at the same distance than the M1 mooring whereas the southern half is over deep water and far from the NW coast line (see Fig. 1).

Figure 20 indicates that three strong downwelling events took place in January and February 1997 as they were linked to strong SE winds. The ocean temperature records at M1 show strong downwelling of warm water. At the same time the warming is sensed around 60 km from Pioneer Seamount on the tomographic track. Both the M1 site and the northern half of the tomographic track were about the same distance from the shelf break. They likely were detecting the same downwelling events. At the same time we see cooling in the southern edge, which was caused by upwelling due to the orientation of the coast in the southern part (see Fig. 1).

The down welling events were observed by the tomographic system as one single intensified event. This was due to the intermittence of the tomographic transmissions that undersampled these events. To make them continuous, the travel time records were smoothed by a low-order polynomial. If the same interpolating polynomial was used to smooth the moored temperature records, one single warming event would have been detected at the M1 site too. To illustrate this, the smoothed M1 temperature data are shown in Fig. 21.

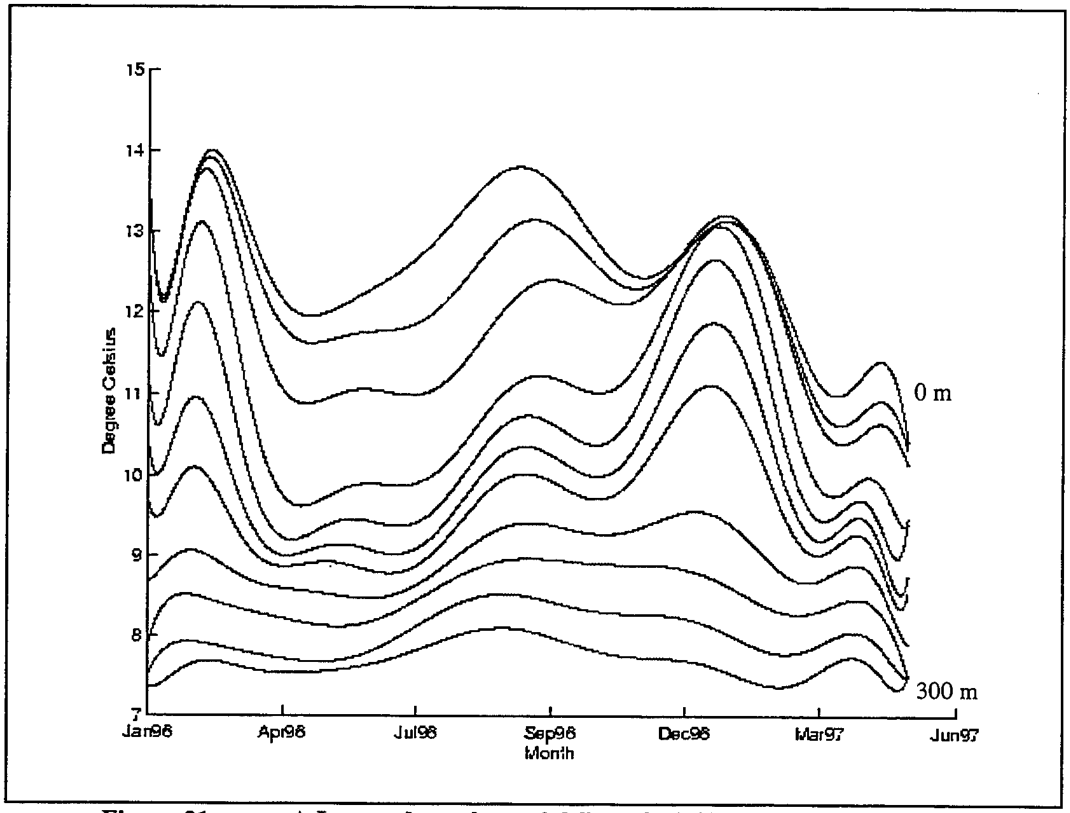

Figure 21. **A Low-order polynomial fit to the M1 temperature records.**

V. CONCLUSIONS

A. SUMMARY OF RESULTS

The electronic emissions of a low-frequency sound source placed by the Acoustic Thermometry of Ocean Climate (ATOC) project on Pioneer Seamount were monitored by a bottom-lying receiver on Sur Ridge from April 1996 to February 1997. The processed signals show a stable arrival pattern that was repeated in all the transmissions during the 11 months. Using the processed data, a tomographic analysis to study the coastal ocean variability along this California transmission path was conducted. The analysis entailed solving the corresponding forward and inverse problems.

In solving the forward problem, a ray-theory approach was used to successfully model the acoustic arrival pattern. Essential to this modeling success was the use a propagation model that can accurately trace raypaths and determine eigenrays in a highly range-dependent coastal environment. Equally essential was the input of a high-quality reference ocean model which was created using measured sound speed profiles and a high-resolution bathymetric data set. The good agreement between the predicted and observed patterns has allowed for the association of the observed peaks with the modeled arrivals and their paths. This model-data association was required to extract the data series of travel time and set up the measurement model for the subsequent inversion.

A linear inversion of the travel-time data with the solution's vertical structure constrained by an EOF resulted in an estimate of the temporal and horizontal variations of the temperature field along the transmission path. The tomographic estimate had a horizontal resolution of about 30 km. It was compared to the temperature and wind measurements from an in situ mooring deployed by the Monterey Bay Aquarium Research Institution (MBARI). The comparison shows that the tomographic estimate is of high quality and that the observed temperature variations were linked to coastal upwelling and downwelling events. This analysis, thus, validates fully the feasibility of using tomography to study coastal temperature variability in the Monterey Bay National Marine Sanctuary on a long-term basis.

B. POTENTIAL IMPROVEMENTS

Without increased investment in the hardware, more frequent emissions will help to avoid interpolation difficulties and improve the resolution of synpotic-scale upwelling and downwelling events. Furthermore, an extended period of transmissions spanning many years will help to study the interannual coastal variability in relation to El Nino events.

LIST OF REFERENCES

Apel, J.R., "*Principal of Ocean Physics*," International Geophysics Series Vol 38, Applied Physics Laboratory, The Johns Hopkins University, Harcourt Brace & Company, 634pp, 1987.

ATOC Instrumentation Group, "Instrumentation for the Acoustic Thermometry of Ocean Climate (ATOC) Prototype Pacific Ocean Network," Oceans '95,3, 1483-1500,1995.

Chiu, C.-S., J.H. Miller and J. F. Lynch, " Inverse Techniques for Coastal Acoustic Tomography," in Environmental Acoustics, D. Lee and M. Schultz, Eds., World Scientific, 1994 a.

Chiu, C.-S., A.J Semtner, , C. M. Ort, J.H. Miller and L.L. Ehret, " A Ray Variability Analysis of Sound Transmission from Heard Island to California" Journal of the Acoustical Society of America, S6,2380-2388, 1994b.

Chiu, C.-S., Department of Oceanography, Naval Postgraduate School, Monterey, CA, Personal Communication, 1995.

Collins, C. A., T. A Rago, J. Steger, "Hydrographic Data Along the California Coast from Pigeon Point to Cape San Martin May through July 1996", Technical Report NPS-OC-97-002 , Naval Postgraduate School, Monterey, January 1997.

Howe, B. M., "Acoustic Thermometry of Ocean Climate (ATOC) : Pioneer Seamount Installation", Applied Physics Laboratory, University of Washington, Technical Memo 3-96, Seattle, April 1996.

John, R. M., J.P. Riley and T. M. Georges, " *HARPO: A Versatile Three-Dimensional Hamiltonian Ray Tracing Program for Acoustic Waves in Ocean with Irregular Bottom*," Wave Propagation Laboratory, National Oceanic and Atmospheric Administration, Boulder, Co, 457 pp., 1986.

Monterey Bay Aquarium Research Institute (MBARI) http://www.mbari.org, F., Chaves , Moss Landing, California.

Munk, W and C. Wunsch, "Ocean Acoustic Tomography: A Scheme for Large Scale Monitoring," Deep Sea Research, Vol. 26A, 123-161, 1979.

Munk, W., P. Worcester, and C. Wunsch, "*Ocean Acoustic Tomography,*" Cambridge University Press, New-York, 1995.

Robinson, I. S., "*Satellite Oceanography*", John Wiley and Sons, New York, 455pp, 1985.

SOAP93, "From Altimetry to Acoustics', http://www.aviso.cls.cnes.fr.,1993.

INITIAL DISTRIBUTION LIST

		No. Copies
1.	Defense Technical Information Center 8725 John J. Kingman Rd., STE 0944 Ft. Belvoir, VA 22060-6218	2
2.	Dudley Knox Library Naval Postgraduate School 411 Dyer Rd. Monterey, CA 93943-5101	2
3.	Professor Robert H. Bourke (Code OC/Bf) Oceanography Department Naval Postgraduate School 883 Dyer Rd., RM 324 Monterey, CA 93943-5122	1
4.	Dr. Ching-Sang Chiu (Code OC/Ci) Oceanography Department Naval Postgraduate School 883 Dyer Rd., RM 324 Monterey, CA 93943-5122	2
5.	Dr. Curtis Collins (Code OC/Co) Oceanography Department Naval Postgraduate School 883 Dyer Rd., RM 324 Monterey, CA 93943-5122	2
6.	Dr. Walter H. Munk UCSD - Scripps Institute of Oceanography 9500 Gilman Dr. IGPP - 0225 La Jolla, CA 92093-0225	1
7.	Dr. Peter Worcester UCSD - Scripps Institute of Oceanography 9500 Gilman Dr. IGPP - 0225 La Jolla, CA 92093-0225	1
8.	CDR John Curtis, N874C Office of the Chief of Naval Operations 2000 Navy Pentagon Washington, DC 20350-200	1

9. Dr. Dennis Conlon 1
IUSS Program Office (PD 80)
SPAWAR
2451 Crystal Drv.
Arlington, VA 22245-5200

10. Dr. Lou Goodman (Code 322PO) 1
Office of Naval Research
800 North Quincy Street
Arlington, VA 22217

11. Dr. Steve Ramp (Code 322PO) 1
Office of Naval Research
800 North Quincy Street
Arlington, VA 22217

12. Dr. Jeff Simmen (Code 321OA) 1
Office of Naval Research
800 North Quincy Street
Arlington, VA 22217

13. Dr. Ellen Livingston (Code 321OA) 1
Office of Naval Research
800 North Quincy Street
Arlington, VA 22217

14. Dr. Bob Gisner 1
Office of Naval Research
800 North Quincy Street
Arlington, VA 22217

15. Dr. Francisco Chavez 1
Monterey Bay Aquarium Research Institute
P.O. Box 628
Moss Landing, CA 95039-0628

16. Dr. Bruce Howe 1
University of Washington / APL
1013 N.E. 40^{th} St.
Seattle, WA 98105

17. Mr. Chris Miller 2
Naval Postgraduate School
589 Dyer Rd. RM 200A
Monterey, CA 93943-5121

18. Ambassade de France 2
Attache Naval
4101 Resevoir Rd. NW
Washington DC, 20007